Avoiding the need to directionally determine the exposure to rainwater penetration for façade designs

José M. Pérez-Bella[a,*], Javier Domínguez-Hernández[a], Enrique Cano-Suñén[a], Juan E. Martínez-Martínez[b], Juan J. del Coz-Díaz[b]

[a] *Department of Construction Engineering, Engineering and Architecture School, University of Zaragoza, María de Luna, s/n, 50018 Zaragoza, Spain.*

[b] *Department of Construction Engineering, University of Oviedo, Edificio Departamental Viesques nº 7, 33204 Gijón, Spain.*

Abstract

The damaging effects caused by the penetration of rainwater into building façades require considering for their design the exposure to the two main climatic factors inducing this penetration: wind-driven rain and the simultaneous wind pressure. The characterisation of these exposures for each possible façade orientation of a building requires analysing exhaustive wind direction records, which significantly increases the calculation effort and prevents calculation in locations without such records. This study examines the possibility to avoid this directional analysis, equally obtaining a functional and reliable exposure characterisation. For this purpose, daily climatic datasets were analysed from 920 weather stations subjected to various environmental and topographic conditions in Mexico, Norway and Spain, and the directional and scalar exposures to wind-driven rain and driving-rain wind pressure were determined at each location. The results show that the maximum directional exposure can be adequately approximated using the scalar exposure value, without the use of wind direction records. Considering the usual constructive practice of using a single façade design for the entire building, this simple and functional characterisation of the expected exposure on the most unfavourable orientation provides a significant support for the design decisions of practitioners.

Keywords

Wind-driven rain; Wind pressure; Façade design; Watertightness; Calculation effort

* Corresponding author. Department of Construction Engineering, University of Zaragoza (UZ), María de Luna, s/n, 50018, Zaragoza, Spain. Tel.Fax: +34 976 76 21 00.
E-mail address: jmpb@unizar.es (José M. Pérez-Bella)

1. Introduction

The watertightness of the façade against rainwater penetration is increasingly being considered in building designs to ensure the durability of enclosures and interior safety conditions and improve the thermal behaviour of buildings [1-4]. To this end, designers must consider the exposure of façades to the climatic factors inducing this penetration: (i) the influx of rainwater, which impacts the façade surface as wind-driven rain (WDR) and (ii) the simultaneous wind pressure (driving-rain wind pressure or DRWP), due to which rainwater advances through the façade by overcoming the surface tension and capillary pressure of the water contained in the porous structure of construction materials [5-7].

The WDR and DRWP exposures depend on the façade orientation according to the prevailing wind directions during precipitation events (an example is shown in Fig. 1). Previous research has identified large exposure differences for different façade orientations of the same building and characteristic directional distribution patterns at each location [8-10]. As a result, wind direction analysis is currently an essential aspect of the calculation, irrespective of the method chosen to determine these climatic exposures, which include experimental studies, numerical simulations based on computational fluid dynamics and semi-empirical approaches [11].

Figure 1. Example of differences in the directional exposure for two weather stations analysed in this study (Itesta and La Posta, both in Mexico); angles are measured in degrees from the North.

Semi-empirical approaches are less accurate than other methods but are nevertheless the most commonly used because of their immediacy of application, functionality and the representativeness of their results under different façade operating conditions [6]. These semi-empirical methods are based on theoretical

formulations that use simultaneous wind and precipitation records collected at each location and empirical adjustments, without requiring exhaustive input data (traditionally, monthly and annual records, and more recently, daily and hourly records) [6,8-9, 12-17].

Thus far, the determination of directional exposures has required a significant calculation effort (a separate calculation is necessary to identify the exposure for every possible façade orientation) and exhaustive records of wind direction at the site. The discontinuity and insufficient age of these wind direction data or their low precision (sometimes limited to the four basic cardinal directions N, S, E and W), constitute a common obstacle to this directional characterisation in many places [9]. Scalar simplifications of this calculation obviate the wind direction and therefore, the directional distribution of the exposure, to provide a single result, which is representative of the overall exposure of the location but inadequate for exposure characterisation in a detailed façade design.

On the other hand, considerations of functionality, economy and simplicity of construction result in the use of a common design for all the façades of the building and only the number, arrangement and size of the openings and the thickness of the thermal insulation are modified according to the solar radiation received by each orientation [18]. Consequently, only the exposure for the most unfavourable orientation is necessary in designing façades against rainwater penetration.

Under these premises, the necessity of performing laborious directional calculations of WDR and DRWP exposures is reassessed, analysing for this purpose the correlation between the scalar exposure and the maximum directional exposure obtained by semi-empirical approaches.

This correlation is evaluated under various climatic and topographic conditions, considering up to 920 locations throughout Mexico, Spain and Norway.

The diversity of the considered exposure conditions enables the general validation of the high degrees of correlation identified, as well as the revaluation of the studies on scalar exposure that have already been performed in various countries and that until now, had a limited utility in detailed design of façades. In

turn, the use of an easily obtainable scalar result to identify the maximum directional exposure (irrespective of its orientation) provides a novel aid for the façade designers. It can also be leveraged to develop more functional design requirements, based on maximum directional exposures that until now could not be determined in many places.

2. Background

To calculate the WDR exposure, the semi-empirical approaches are based on an overall formulation designated as the 'WDR relationship' (Eq. 1), which multiplies simultaneous records of the wind speed U (m/s) and the rainfall intensity R_h (mm) [19-20]. The empirical coefficient k (s/m) depends on the façade geometry, the building configuration, the size distribution of raindrops and the U and R_h values [21]. A cosine projection of the simultaneous records of the wind direction D (º) and the analysed façade orientation θ (º) is used to determine the directional exposure WDR_θ (l/m^2 or mm) [6]. Consequently, a different calculation must be performed for every possible façade orientation, which increases the calculation effort of the procedure (the possible façade orientations are usually analysed at intervals of 15º to 90º) [9, 12, 22-23].

$$WDR_\theta = k \cdot U \cdot R_h \cdot \cos\left(D - \theta\right) \quad (1)$$

This WDR relationship has been developed in the standard ISO 15927-3, wherein empirical adjustment coefficients are introduced to incorporate hourly climatic data (Eq. 2). The average annual value of WDR exposure on a specific façade is determined by considering only the m climatic records gathered over N years for which the wind direction D blows against an orientation θ of the façade [24]. Dimensionless coefficients are incorporated in the standard to represent the interactions among wind, rain and the building, thereby weighting the effects of shape, terrain roughness, surrounding topography and nearby obstructions of the façade on the WDR exposure.

$$WDR_{\theta} = \frac{2}{9} \cdot \frac{\sum_{i=1}^{m} U_i \cdot \left(R_{h\,i}\right)^{8/9} \cdot \cos\left(D_i - \theta\right)}{N} \tag{2}$$

However, the usual lack of hourly records compiled over long periods and the indeterminacy of the aforementioned empirical coefficients for different climatic conditions and other climatic data (daily or monthly) have popularised a simpler characterisation, known as the annual Driving Rain Index (Eq. 3). This directional $aDRI_{\theta}$ value ($m^2/s \cdot yr$) can be calculated from m daily ($daDRI_{\theta}$), monthly ($maDRI_{\theta}$), annual ($aaDRI_{\theta}$) ... records collected over N years at the respective location. Only the records for which rain affects the analysed orientation (i.e., the positive cosine projection) are considered in the summation. Thus, the façades oriented towards the prevailing storm winds may be subject to high average exposures, even greater than the average scalar exposure that would be obtained by omitting this cosine projection.

As can be expected, the use of climate records obtained over exhaustive intervals of time (e.g., 10-min records) increases the accuracy of this exposure characterisation via a more precise representation of the simultaneity of wind and precipitation that produces the influx of rainwater over the façade [25-28]. Despite its simplicity, this index can be adjusted using coefficients k, which may be generic or empirically determined under site-specific operating conditions [29].

$$aDRI_{\theta} = \frac{\sum_{i=1}^{m} U_i \cdot \left(\frac{R_{h\,i}}{1000}\right) \cdot \cos\left(D_i - \theta\right)}{N} \tag{3}$$

An aDRI value can be determined at locations for which wind direction records are not available by disregarding the cosine projection and considering all of the available records during precipitation events. The resulting scalar result $aDRI$ ($m^2/s \cdot yr$) only characterises the overall WDR exposure at the considered location, without differentiating the exposure over each façade orientation. However, the possibility of performing this calculation in a large number of places makes these scalar analyses broader and more common than the directional ones [6, 13-17].

An analogous calculation can be performed for the DRWP exposure using wind velocity records that are concurrent with significant precipitation events (i.e., rainfall amount > 0.05 mm) collected at each location. DRWP analysis has traditionally received much less attention than WDR exposure. Thus, the lack of DRWP analyses in most countries prevents an exhaustive assessment of the risk of water penetration on building façades, even when WDR studies are available [7, 15, 17].

In the few studies in which the DRWP has been calculated, the Bernoulli equation (Eq. 4) has been used in conjunction with the m wind records that affect the orientation θ of the façade, the pressure coefficient C_p (-) and the air density ρ_{air} (kg/m^3) [8, 15]. The cosine projection is used in the directional calculation of $DRWP_\theta$ (Pa), which also requires a specific study for each possible façade orientation θ and wind direction data that are not always available.

$$DRWP_\theta = \frac{\sum_{i=1}^{m} C_p \cdot \frac{1}{2} \cdot \rho_{air\ i} \cdot U_i^{\,2} \cdot \cos\left(D_i - \theta\right)}{m} \tag{4}$$

The calculation is usually simplified by assuming a conservative value of unity for C_p and an air density value of 1.2 kg/m^3. As in the aDRI calculation, the cosine projection can be omitted to obtain a scalar result that is independent of the façade orientation. Annual ($aDRWP_\theta$), monthly ($mDRWP_\theta$) and daily ($dDRWP_\theta$) records can also be used. The more exhaustive the record intervals are, the higher the accuracy of the results.

Next, the WDR and DRWP exposures are analysed at 920 weather stations using daily climate records of the precipitation and the simultaneous wind velocity (i.e., wind speed and direction). The directional and scalar daDRI and dDRWP values are calculated to identify correlations from which the maximum directional exposure can be extrapolated using only the scalar result at the considered location.

To the best of the authors' knowledge, this research study is the most comprehensive on this subject, both in terms of the number of stations analysed and the variety of climatic, topographic and exposure conditions represented (previously, only partial conclusions from six Chilean and six Spanish sites had

been reached) [9, 28]. The aim of this study is to propose a new approach that substantially modifies the means by which WDR and DRWP exposures are determined to facilitate façade designs (by circumventing the laborious directional calculation) and enable detailed exposure characterisation even at locations without wind direction records.

3. Analysis of scalar and directional exposures

To achieve the study objective, three countries (Mexico, Norway and Spain) were selected that are characterised by diverse climatic conditions and for which there is free access to climatic data, with a reasonable age and a daily frequency, at multiple locations. The 920 analysed stations are distributed across the three countries, and the average age of the climate records is approximately 8.4 years (Table 1). Daily data from climatic records of significant precipitation (> 0.05 mm directly collected through rain gauges) and wind velocity (speed and direction) were used that were recorded at a height of 10 m above ground level in an open field (airfield conditions). In some cases, these consulted daily values have been produced by automatic weather stations, applying the criteria of the Word Meteorological Organization to raw data gathered at shorter intervals [30]. Stations with less than two years of complete records have not been considered, nor those years with more than 10% of missing data. This threshold was extended to 15% in some stations in Mexico due to the greater discontinuity of their records (primarily wind direction data), thus considering a greater number of stations. Finally, no data have been filled up: if one of the three daily variables was missing, that day was omitted.

These data were used to determine the $daDRI_\theta$ and $dDRWP_\theta$ values that define the risk of rainwater penetration into the façades (Eqs. 3 and 4), considering 15º intervals for the possible façade orientations θ and constant values for C_p and ρ_{air} (as mentioned above). The analysis for each location was completed using the scalar exposures obtained by omitting the cosine projection in Eqs. 3 and 4.

Table 1.
Characteristics of 920 stations considered in this study.

3.1 Exposure results

The majority of the analysed stations are located in Mexico (516), where the highest altitudes are also reached (up to 2,771 m for the weather station of Melchor Ocampo, near Mexico City). In general, the records available through the Mexican Institute of Forestry, Agriculture and Livestock Research are of a lower quality than those from the other countries studied, with an average age that does not exceed seven years and an uneven distribution of stations in the territory (see Fig. 2) [31]. Stations with less than two full years of available climate records were excluded from the study. As a result, the Mexican states of Nayarit, Jalisco, Colima, Michoacán, Querétaro and Tabasco had to be omitted given the poor representativeness of their available climatic records.

The country has a very diverse climate that ranges from a tropical rainforest climate in the states of Chiapas, Veracruz and Oaxaca to hot desert climates in Sonora, Baja California and other northern regions [32]. In general, more extreme temperatures can be found north of the 24ºN latitude, where the low rainfall amount only increases around the mountain range of the Sierra Madre Occidental. The mean annual rainfall progressively increases southward and is highest near the coasts and in the southeast of the country [33]. The most intense winds are also observed in the coastal areas, mainly because of the seasonal action of tropical cyclones that form over the Atlantic and Pacific oceans [34-35].

Figure 2. Geographical scope of this study: analysed stations are shown by crosses.

The proximity of two oceans around the Isthmus of Tehuantepec produces extreme rainfall and wind conditions, making the nearby stations of La Mina in Oaxaca and Itesta, Cosamaloapan and La Posta in Veracruz the most exposed to WDR among all of the analysed locations (Table 2). By contrast, most Mexican stations have comparatively low WDR exposure values, resulting in an average daDRI (scalar value) of only 1.2 $m^2/s \cdot yr$, the lowest of the countries studied (e.g., Valle de Mulegue, Pozo Peña and Ejído Díaz Ordaz stations, all of which are in Baja California Sur, do not exceed 0.05 $m^2/s \cdot yr$).

Table 2.
Mexican stations with highest WDR exposure (daDRI values).

The stations of Itesta, La Granja, Sagitario, Álamo, La Posta and La Conquista, all of which are in Veracruz region, are subjected to the highest wind pressures during precipitation events (Table 3). Overall, the sites around the Isthmus of Tehuantepec (especially along the Atlantic slope) are at the greatest risk of rainwater penetration into façades because of the water influx and the wind pressure that drives this water through building materials. By contrast, the northern and central Mexican sites generally have very low DRWP exposures, where the average scalar value does not exceed 5.7 Pa.

Table 3.
Mexican stations with highest DRWP exposure (dDRWP values).

The 107 Norwegian stations are subjected to very different conditions from the Mexican sites (altitudes not exceeding 1,210 m and latitudes up to 78.9º N, as in Ny-Alesund, Svalbard archipelago) and present very high exposures. The climate in Norway varies from oceanic on the southeast coast, including a warm-summer continental climate around Oslo and hemiboreal climates in the Nord-Trøndelag region, to

subarctic and tundra climates in the north and the mountainous centre [32]. There is a higher number of weather stations in the south (Fig. 2), with only a few isolated stations in the northernmost regions, including the Svalbard archipelago, the islands of Hopen, Bjornova and Jan Mayen and the area north of the Scandinavian Peninsula.

Most stations have 10 years of climate records, which are accessible through the Norwegian Meteorological Institute [36]. The rainfall amount is very high along the entire Atlantic coast (above 2,000 mm/yr) and decreases towards the east of the country to below 500 mm/yr in some areas. Extreme weather conditions in the North Sea and the Norwegian Sea also produce very strong winds, which increase the risk of water penetration into façades, except in the more protected regions of the southeast [35, 37]. Thus, the average daDRI (scalar value) of the analysed stations reaches 4.1 $m^2/s \cdot yr$ (the highest among the analysed countries) and nine stations along the southwest coast surpass 10 $m^2/s \cdot yr$ (Table 4). The highest WDR exposure of 13.21 $m^2/s \cdot yr$ is identified at the Ona II station (More Og Romsdal region), where the directional maximum reaches 9.20 $m^2/s \cdot yr$ at an orientation of 225º from North.

Table 4.
Norwegian stations with highest WDR exposure (daDRI values).

Although the wind pressure during precipitation is never as high as at the Mexican stations subject to tropical cyclones, the highest average value of dDRWP among the three countries is also found (scalar value of 12.4 Pa). The most exposed stations are mostly located near the Atlantic coast (Table 5).

Table 5.
Norwegian stations with highest DRWP exposure (dDRWP values).

Lastly, the 297 Spanish stations are located at latitudes intermediate between those of Mexico and Norway, with an average altitude of 403 m and a maximum altitude of 1,495 m in Hornos de Moncalvillo in the Iberian System mountain range. The climatic data obtained from these stations are of good quality, with an average age above 10 years and a distribution that ensures the uniform characterisation of the entire territory. The climatic data were collected by the Spanish Meteorological Agency (AEMET), the Spanish Agroclimatic Information System and various Spanish regional institutions [38-40].

The Spanish climate exhibits significant diversity, with an oceanic climate in the northern areas around the Bay of Biscay, a Mediterranean hot summer climate in much of the centre and the south and even arid and semi-arid desert climates southeast of the Iberian Peninsula [32]. Precipitation decreases significantly towards the southeast, from more than 1,500 mm/yr along the northwest coast to below 200 mm/yr in the arid and semi-arid areas. Although some areas are subject to intense winds (e.g., the Strait of Gibraltar, the North coast and the Ebro river valley), wind conditions in Spain are generally more uniform and moderate than in Mexico and Norway [41].

Thus, the stations with the highest WDR exposure are located along the mountainous northern coast (Table 6), especially in the Basque Country region (Machichaco, 11.29 $m^2/s \cdot yr$; La Cerroja and Jaizquíbel, above 9 $m^2/s \cdot yr$). However, the low precipitation over much of Spain results in an average scalar daDRI of only 1.6 $m^2/s \cdot yr$ (i.e., close to the Mexican average). In fact, the scalar daDRI do not exceed 0.5 $m^2/s \cdot yr$ for 43 stations (approximately 15% of the total number of Spanish stations analysed).

Table 6.
Spanish stations with highest WDR exposure (daDRI values).

The stations along the northern coast of the country are also subject to high DRWP exposure because of strong coastal winds and high altitudes (Table 7). However, Spanish stations have the lowest mean

DRWP exposure of the countries analysed (the average scalar dDRWP is 4.3 Pa and only 22 stations, 7.4% of those evaluated, exceed 10 Pa). Thus, Spanish stations complete the database of the study with the stations of lowest DRWP exposure.

Table 7.
Spanish stations with highest DRWP exposure (dDRWP values).

3.2 Correlation between scalar and maximum directional exposures

All the exposure results obtained for the 920 analysed locations are used to determine the best-fit correlation between the scalar and maximum directional exposures (for both the WDR and the DRWP exposures). Despite the variety of climates, topographic conditions and represented exposures that have been briefly described, the high coefficients of determination found validate a clear correlation between both magnitudes that can be used to extrapolate the directional result from the scalar value (Fig. 3). Similar results can also be obtained if the 50 stations with less than 5 years of records are dismissed (less than 5.5% of the total). The correlations are not invalidated by the especially dry or rainy nature of the years considered, since similar results are obtained in both desert and humid climates. However, this fact should be considered for the detailed design of façades in locations with few years of records, given the low representativeness of the initial scalar exposure. As seen, these extrapolations can obtain negative directional results; although only in locations where the exposure can be considered negligible for the façade design (scalar daDRI values < 0.09 $m^2/s \cdot yr$ and scalar dDRWP values < 0.67 Pa).

Figure 3. Best-fit correlation between scalar and maximum directional exposures for 920 analysed locations. *Percent error range of ± 20% is also shown.*

The percent error range incorporated in Fig. 3 allows interpreting the distance between the station results and the best-fit correlation (even by exposure range). As seen, the error remains below 20% for high exposures and in most stations, although larger errors can be identified by reducing the exposure (the quantitative error also decreases analogously).

Considering the two locations presented in Fig. 1, the maximum directional exposures could be extrapolated using only the scalar exposures. For Itesta station, a scalar daDRI value of 19.05 $m^2/s \cdot yr$ (Table 2) is calculated, and then the identified correlation is used to extrapolate a maximum directional value of 12.51 $m^2/s \cdot yr$, which is reasonably close to the 11.99 $m^2/s \cdot yr$ determined by the laborious directional calculation. Similarly, for La Posta station (for which the calculated scalar daDRI is 14.20 $m^2/s \cdot yr$), the extrapolated directional maximum of 9.31 $m^2/s \cdot yr$ is comparable to the 10.55 $m^2/s \cdot yr$ identified by the directional analysis. Note that both stations are among the most exposed, which increases the quantitative errors incurred (0.52 and 1.24 $m^2/s \cdot yr$ for Itesta and La Posta, respectively). However, the corresponding percentage errors are merely 4.3% and 11.8%.

Likewise, the scalar DRWP exposure for Itesta (238.50 Pa, see Table 3) is used to extrapolate a maximum directional exposure of 267.23 Pa, which is very close to the directional analysis result of 266.39 Pa, corresponding to a 0.3% error. The scalar dDRWP of 122.40 Pa for La Posta produces an estimated directional maximum of 136.78 Pa, compared to 147.18 Pa calculated by the laborious directional analysis (7.1% error).

The aforementioned results show that the identified correlation can be used to quickly and functionally approximate the sole exposure of usual interest in building façade design, which is the value of the most exposed façade. This approximate value obviates the aforementioned laborious directional analysis, substantially simplifying façade design and enabling a reasonable characterisation of the WDR and DRWP exposures even for locations without wind direction records. The large number of locations

analysed and the associated geographic and climatic variety favour the representativeness of the identified correlations. In turn, the scalar exposure results that are already available for other countries (e.g., Brazil, China, Greece, India, Nigeria, Turkey among many others) could be extrapolated, thus increasing the current interest of these studies for the detailed design of façades [6, 13-14, 16 -17, 42-43]. This functionality also opens the door to improve current performance-based building codes, in which precisely, to identify the maximum exposure by location is a key factor in defining specific performance requirements. Such is the case of the three countries analysed, in which the façade design is conducted based on a generic qualitative requirement (Mexico and Norway), or based on unreliable quantitative requirements (Spain) [15, 44-45].

4. Discussion and relevant factors for identified correlations

Although high coefficients of determination are obtained, Fig. 3 shows how the extrapolation process produces location-dependent errors that are generally lower than 20%. The typical use of safety factors reduces the effect of these errors on façade design; nevertheless, the potential influence of climatic and dataset time resolution factors over both correlations is analysed below.

4.1 Regional and climatic factors

The influence of the exposure value on the identified correlations is analysed by grouping the stations by exposure range (Table 8). The limits of these exposure ranges are based on traditionally accepted scalar aDRI values that were established by Lacy in 1962 [19]. In the absence of internationally accepted classifications for DRWP exposure, the thresholds have been adopted while maintaining a number of stations per range that is similar to that obtained for WDR exposure. In general, these ranges group a smaller number of stations when more severe exposures are considered.

Table 8.
Distribution of analysed locations for different exposure ranges by country.

The Norwegian stations are subjected to the most adverse conditions of the three countries and up to 52.3% of these stations present moderate, high or severe WDR exposure. Spain has fewer severely exposed locations than Mexico but has a higher number of stations with moderate WDR exposure (approximately 13% of the total number of locations in Spain). The Mexican stations are generally located in sheltered areas, except for those on the coast of the Gulf of Mexico and around the Isthmus of Tehuantepec (35 of the 521 stations analysed), which are subjected to the periodic action of extreme climatic phenomena. The four most exposed stations among the 920 analysed stations are located in these Mexican areas.

Regarding the DRWP exposure, Norway has a more unfavourable climatology than Spain and Mexico, and scalar dDRWP values above 8.5 Pa are obtained at up to 48 of the 107 Norwegian stations. By contrast, the stations in Spain and Mexico have much lower exposures, and the scalar dDRWP values at almost 90% of their stations are below the aforementioned threshold. However, a significantly higher number of Mexican sites are subjected to severe exposures (i.e., scalar dDRWP values above 45 Pa) than in Spain (1.7% in Mexico vs. 0.3% in Spain).

Very high coefficients of determination are also identified for the country-specific correlations (Fig. 4). In addition, very similar correlations were obtained for the three countries, despite their notable climatic, topographic and exposure differences. This result reconfirms the general validity of the extrapolation procedure to obtain the maximum directional exposures from the scalar values. Thus, although region-specific correlations could be used, the general correlation maintains reasonable validity for any geographical area. Evidently, the analysis of more countries, new stations or a greater number of years of records can refine these general and country-specific correlations. Therefore, it would be advisable to

broaden the scope of the study in the future, in order to provide even more representative correlations or particular correlations for specific areas of each country.

Figure 4. Best-fit correlation between scalar and maximum directional exposures by country.

The most significant inaccuracies in the general WDR correlation are incurred for locations in Mexico (La Granja, Veracruz; El Porvenir, Oaxaca) and Spain (La Cerroja and Belauntza, Basque Country; Carreña de Cabrales, Asturias), where the maximum $daDRI_{\theta}$ values are typically higher than the extrapolated exposure. For its part, the stations for which the most inaccurate extrapolations were obtained are located around the Isthmus of Tehuantepec (Ozulama and Cosamaloapan in Veracruz; Yetla in Oaxaca). A detailed analysis reveals similar climatic and topographic conditions for all of these sites: tropical cyclones in Mexico and intense coastal winds channelled through mountain valleys in Spain. Both situations appear to increase the concentration of WDR on certain façade orientations, resulting in maximum directional exposures that are slightly higher than extrapolated ones.

4.2 Dataset time resolution factor: correlation obtained using hourly data (ISO 15927-3)

As discussed above, the accuracy of the semi-empirical exposure indices is conditioned by the time resolution of the climate dataset. Thus, the accuracy of the results decreases with the exhaustiveness of the records used in Eqs. 3 and 4. The daily records that are used in this study cannot reproduce instantaneous simultaneity between precipitation and the wind velocity; therefore, the scalar results in Tables 2-7 can be adjusted before being used in façade designs.

In previous studies, the mean error incurred by the use of daily data has been quantified by comparison to the results obtained using 10-min data: errors of 8.15% in the scalar daDRI values and 37.62% in the scalar dDRWP values have been reported. Corresponding dispersions of up to 4.0% and 10.7% have been calculated. Despite being preliminary in nature (only six stations in northwest Spain were analysed), these studies provide an initial guideline for adjusting the scalar results obtained in the present study to produce more reliable exposure values (Eqs. 5 and 6) [27].

$$_{10-\min} aDRI = 1.152 \cdot daDRI - 0.234 \quad \left(R^2 = 0.990;\ \text{for 6 Spanish stations}\right) \tag{5}$$

$$_{10-\min} DRWP = 1.852 \cdot dDRWP - 1.568 \quad \left(R^2 = 0.975;\ \text{for 6 Spanish stations}\right) \tag{6}$$

To rule out the possible influence of dataset time resolution on the validity of these correlations, a WDR analysis based on hourly climatic data is performed by using the formulation established by the ISO standard 15927-3 (Eq. 2) [24].

The reduced availability of hourly data restricts the analysis set to a group of 40 Spanish stations, with hourly records compiled between 2008 and 2018 (10 years) [40]. All of these stations are located in the northwest Iberian Peninsula, which is one of the most exposed areas of Spain, given its proximity to the coast of the Atlantic Ocean (Galicia region). Despite the geographical proximity of these stations, the calculated mean annual WDR exposure reveals significant variations (the maximum WDR_θ values range from 255 mm/yr in Verín to 3,994 mm/yr in Lousame). The altitudes of the stations range from 3 m at the coastal stations to 1,758 m at the Manzaneda station. Thus, the selected stations are representative of significantly diverse environmental and topographical conditions.

In turn, the obtained scalar WDR exposure at each site (omitting the cosine projection in Eq. 2) is used to identify a correlation between the scalar and maximum directional exposures. These results are shown in Table 9 (only the higher WDR_θ values are presented for conciseness). The complete results are presented in the supplementary material for this paper. The WDR correlation for these Spanish locations (Fig. 5) has

a high coefficient of determination (R^2 equals 0.9667), which is even higher than previously obtained using daily climatic records.

Table 9.
Scalar and maximum directional WDR exposures calculated using ISO standard 15927-3 for Northwestern Spain (Galicia region).

Figure 5. Best-fit correlation between scalar and maximum directional WDR exposures for 40 Spanish sites based on hourly data (according to ISO 15927-3). *Percent error range of ± 20% is also shown*.

All of the results presented above validate a clear correlation between the scalar and maximum directional exposures under various environmental conditions and dataset time resolutions, which can be used to simply approximate the most unfavourable rainwater penetration condition on the façades of the building. In turn, the scalar starting data (already available in many regions or easily calculable), can be adjusted using Eqs. 5 and 6 or through other identified relationships between the WDR and DRWP exposures calculated from daily, monthly and even annual data [6, 9, 13-14, 16-17]. In that case, it should be taken into account that the sequence of statistically produced functions could lead to accumulated errors and therefore, to largely differ from reality results.

5. Conclusions

In this study, the exposures for rainwater penetration into building façades were analysed for a large number of locations under various climatic and topographic conditions. The results demonstrated the

existence of a clear correlation between the scalar WDR and DRWP exposures at these locations and the corresponding maximum directional exposures for specific façade orientations.

The ability to easily approximate the exposure at the most unfavourable façade from the associated scalar exposure represents a novel alternative to the traditional determination of WDR and DRWP exposures, which involves laborious directional calculations that cannot be realised for many sites. This extrapolation reduces the computational intensiveness of façade design and provides support for the decisions of practitioners, even in locations at which climatic records are limited.

This advance in the field can be used to reassess scalar exposure results that are already available for many regions, which from now on will allow extrapolating the most unfavourable exposure in a facile and functionally way for its use in the design of any building façade (without increasing the practitioner's effort). The simplicity of the approach presented here also facilitates incorporation into building codes and enables the establishment of design requirements based on these maximum directional exposures applicable to the entire territory.

This extrapolated directional result can be adjusted in the usual way to account for different façade shapes, terrain roughness, surroundings and other dataset time resolutions: however, the adoption of additional precautions (e.g., safety factors) is recommended for sites subjected to specific environmental conditions, including strong winds that are channelled through mountainous valleys or recurrent and large-scale storm systems, such as tropical cyclones.

Acknowledgements

This research was partially funded by the Foundation for the Promotion of Applied Scientific Research and Technology in Asturias (FICYT) through the GRUPIN project Ref. IDI/2018/000221, and The Spanish Ministry of Science, Innovation and Universities through the State Plan for Scientific and

Technical Research and Innovation with the project Ref. PGC2018-098459-B-I00, both co-financed with EU FEDER funds. A part of the results was obtained from information provided by the Spanish Meteorological Agency, Ministry of Agriculture, Food and Environment (AEMET). The authors acknowledge engineers J.M. Esteban Samitier, G.M. Farina García, A. Ferrer Ferrer, P. Guallar García, M. Hernando Serrano, M. Martín Alcubierre, J.M. Monasterio Barricarte, S. Pérez Acín, A. Ruiz Cartiel and A. Santiago Ciprián, for their help with data collection and processing.

References

[1] WHO, Environmental burden of disease associated with inadequate housing - Methods for quantifying health impacts of selected housing risks in the WHO European region, World Health Organization, Copenhagen, 2011.

[2] C. Hall, W.D. Hoff, Water transport in brick, stone and concrete, second ed., Spon Press, New York, 2012.

[3] A. Erkal, D. D'Ayala, L. Sequeira, Assessment of wind-driven rain impact, related surface erosion and surface strength reduction of historic building materials, Build. Environ. 57 (2012) 336–348. https://doi.org/10.1016/j.buildenv.2012.05.004

[4] V. Kočí, E. Vejmelková, M. Čáchová, D. Koňáková, M. Keppert, J, Maděra, R. Černý, 2017. Effect of moisture content on thermal properties of porous building materials, Int. J. Thermophys. 38:28. https://doi.org/10.1007/s10765-016-2164-8

[5] EN 12865, Hygrothermal performance of building components and building elements. Determination of the resistance of external wall systems to driving rain under pulsating air pressure, European Committee for Standardization Brussels, 2001.

[6] B. Blocken, J. Carmeliet, A review of wind-driven rain research in building science, J. Wind. Eng. Ind. Aerodyn. 92-13 (2004) 1079–1130. https://doi.org/10.1016/j.jweia.2004.06.003

[7] S.M. Cornick, M.A. Lacasse, A review of climate loads relevant to assessing the watertightness performance of walls, windows, and wall-window interfaces, J. ASTM. Int. 2-10 (2005) 1–16. https://doi.org/10.1520/JAI12505

[8] R.E. Welsh, W.R. Skinner, R.J. Morris, A climatology of driving rain pressure for Canada (Climate and Atmospheric Research Directorate draft report), Environment Canada, Atmospheric Environment Service, Gatineau, 1989.

[9] J.M. Pérez, J. Domínguez, E. Cano, J.J. del Coz, M. Alonso, Global analysis of building facade exposure to water penetration in Chile, Build. Environ. 70 (2013) 284-297. http://dx.doi.org/10.1016/j.buildenv.2013.09.001.

[10] H. Ge, U.K. Deb Nath, V. Chiu, Field measurements of wind-driven rain on mid- and high-rise buildings in three Canadian regions, Build. Environ. 116 (2017) 228–245. https://doi.org/10.1016/j.buildenv.2017.02.016

[11] B. Blocken, J. Carmeliet, Overview of the three state-of-the-art wind-driven rain assessment models and comparison based on model theory, Build. Environ. 45 (2010) 691-703. https://doi.org/10.1016/j.buildenv.2009.08.007

[12] J.S. Underwood, V. Meentemeyer, Climatology of wind-driven rain for the contiguous United States for the period 1971 to 1995, Phys. Geogr. 19-6 (1998) 445–462. https://doi.org/10.1080/02723646.1998.10642661

[13] I. Chand, P.K. Bhargava, Estimation of driving rain index for India, Build. Environ. 37-5 (2002) 549–554. https://doi.org/10.1016/S0360-1323(01)00057-9

[14] F.O.A. Akingbade, Estimation of driving rain index for Nigeria, Archit. Sci. Rev. 47-2 (2004) 103–106. https://doi.org/10.1080/00038628.2004.9697032

[15] J.M. Pérez, J. Domínguez, B. Rodríguez, J.J. del Coz, E. Cano, Combined use of wind-driven rain and wind pressure to define water penetration risk into building facades: the Spanish case, Build. Environ. 64 (2013) 46–56. https://doi.org/10.1016/j.buildenv.2013.03.004

[16] C. Giarma, D. Aravantinos, On building components' exposure to driving rain in Greece, J. Wind. Eng. Ind. Aerodyn. 125 (2014) 133–145. https://doi.org/10.1016/j.jweia.2013.11.014

[17] J. Domínguez, J.M. Pérez, M. Alonso, E. Cano, J.J. del Coz, Assessment of water penetration risk in building facades throughout Brazil, Build. Res. Inf. 45-5 (2016) 1-16. https://doi.org/10.1080/09613218.2016.1183441

[18] R. Pacheco, J. Ordóñez, G. Martínez, Energy efficient design of building: a review, Renew. Sustain. Energy. Rev. 16 (2012) 3559–3573. https://doi.org/10.1016/j.rser.2012.03.045

[19] S. Hoppestad, Slagregninorge (Driving rain in Norway, in Norwegian); NBI Report no. 13, Norwegian Building Research Institute, Oslo, 1955.

[20] R.E. Lacy, H.C. Shellard, An index of driving rain, Meteorol. Mag. 91-1080 (1962) 177–184.

[21] J.F. Straube, E.F.P. Burnett, Simplified prediction of driving rain deposition, in: Proceedings of international building physics conference, Eindhoven, 2000, pp. 375–382.

[22] J.P. Rydock, A. Gustavsen, A look at driving rain spells at three cities in Great Britain, Build. Environ. 42 (2007) 1386–1390. https://doi.org/10.1016/j.buildenv.2005.11.020

[23] H. Ge, R. Krpan, Wind-driven rain study in the coastal climate of British Columbia (Final report). British Columbia Institute of Technology, Burnaby, 2009.

[24] EN ISO 15927-3, Hygrothermal performance of buildings. Calculation and presentation of climatic data. Part 3: calculation of a driving rain index for vertical surfaces from hourly wind and rain data, European Committee for Standardization, Brussels, 2009.

[25] B. Blocken, J. Carmeliet, Guidelines of the required time resolution of meteorological input data for wind-driven rain calculations on buildings, J. Wind. Eng. Ind. Aerodyn. 96 (2008) 621-639. https://doi.org/10.1016/j.jweia.2008.02.008

[26] H. Ge, Influence of time resolution and averaging techniques of meteorological data on the estimation of wind-driven rain load on building facades for Canadian climates, J. Wind. Eng. Ind. Aerodyn. 143 (2015) 50–61. https://doi.org/10.1016/j.jweia.2015.04.019

[27] J.M. Pérez, J. Domínguez, E. Cano, J.J. del Coz, M. Alonso, On the significance of the climate-dataset time resolution in characterising wind-driven rain and simultaneous wind pressure. Part I: scalar approach, Stoch. Environ. Res. Risk. Assess. 32 (2018) 1783-1797. https://doi.org/10.1007/s00477-017-1479-8

[28] J.M. Pérez, J. Domínguez, E. Cano, J.J. del Coz, F.P. Álvarez, On the significance of the climate-dataset time resolution in characterising wind-driven rain and simultaneous wind pressure. Part II: directional analysis, Stoch. Environ. Res. Risk. Assess. 32 (2018) 1799-1815. https://doi.org/10.1007/s00477-017-1480-2

[29] Henriques FMA. Quantification of wind-driven rain. An experimental approach. A general review on driven rain and details of an experiment in Portugal to supplement existing research results in Norway, the UK and elsewhere. Build Res Inf 1992; 20(5):295-2977. http://dx.doi.org/10.1080/09613219208727227.

[30] WMO, Guide to Meteorological instruments and methods of observation (WMO-No 8), World Meteorological Organization, Geneva, 2008.

[31] Mexican Institute of Forestry, Agriculture and Livestock Research, National Modeling and Remote Sensing Laboratory Daily climatic data. https://clima.inifap.gob.mx/lnmysr/Estaciones, 2019 (accessed 29 November 2019).

[32] M.C. Peel, B.L. Finlayson, T.A. Mcmahon, Updated world map of the Köppen-Geiger climate classification, Hydrol. Earth. Syst. Sci. 11 (2007) 1633-1644. https://doi.org/10.5194/hess-11-1633-2007

[33] Mexican National Meteorological Service, Climatology. https://smn.cna.gob.mx/es/climatologia/informacion-climatologica/mapas-de-climatologia-1981-2010, 2019 (accessed 29 November 2019).

[34] J. Larson, Y. Zhou, R.W. Higgins, Characteristics of landfalling tropical cyclones in the United States and Mexico: Climatology and interannual variability, J. Climate. 18 (2005) 1247-1262. https://doi.org/10.1175/JCLI3317.1

[35] Global Wind Atlas. https://globalwindatlas.info/, 2019 (accessed 29 November 2019).

[36] Norwegian Meteorological Institute, eKlima. http://sharki.oslo.dnmi.no/portal/page?_pageid=73,39035,73_39049&_dad=portal&_schema=PORTAL, 2019 (accessed 29 November 2019).

[37] Norwegian Water Resources and Energy Directorate, SeNorge - Normal annual precipitation (1971-2000). http://www.senorge.no/?p=klima, 2019 (accessed 29 November 2019).

[38] Spanish Meteorological Agency (AEMET), Service request. https://sede.aemet.gob.es/AEMET/es/GestionPeticiones/solicitudes, 2019 (accessed 29 November 2019).

[39] Spanish Agroclimatic Information System, Data access. http://eportal.mapama.gob.es/websiar/SeleccionParametrosMap.aspx?dst=1, 2019 (accessed 29 November 2019).

[40] Government of Galicia, Department of Environment, Territory and Housing (data access). https://www.meteogalicia.gal/observacion/rede/redeIndex.action?request_locale=es, 2019 (accessed 29 November 2019).

[41] National Center for Geographic Information, National Atlas of Spain - Section II: The land environment, climatology. http://www.ign.es/ane/ane1986-2008/, 2019 (accessed 29 November 2019).

[42] N. Sahal, Proposed approach for defining climate regions for Turkey based on annual driving rain index and heating degree-days for building envelope design, Build. Environ. 41-4 (2006) 520-526. https://doi.org/10.1016/j.buildenv.2005.07.004

[43] P. Sauer, An annual driven rain index for China, Build. Environ. 22-4 (1987) 239-240. https://doi.org/10.1016/0360-1323(87)90016-3

[44] Directorate for Construction Quality, Byggteknisk forskrift TEK17 (Technical Construction Regulation TEK17, in Norwegian). Section 13-9. https://dibk.no/byggereglene/byggteknisk-forskrift-tek17/ (accessed 2 March 2020).

[45] Goverment of Mexico. Código de edificación de la vivienda 2017 (Dwelling Building Code 2017, in Spanish). Section 3001.2. https://www.gob.mx/cms/uploads/attachment/file/320345/CEV_2017__FINAL_.pdf (accessed 2 March 2020).

List of tables

Table 1.
Characteristics of 920 stations considered in this work.

	México	**Norway**	**Spain**	**Total**
Number of stations	516	107	297	920
Min. altitude (m)	3	3	3	
Max. altitude (m)	2771	1210	1495	
Avg. altitude (m)	1222	188	403	679
Min. latitude (DD)	+14.7	+58.0	+27.8	
Max. latitude (DD)	+32.5	+78.9	+43.7	
Avg. latitude (DD)	+23.9	+63.1	+39.6	+33.6
Years of data	Stations	Stations	Stations	
2	6	-	20	26
3	4	-	-	4
4	18	-	2	20
5	138	-	22	160
6	89	-	13	102
7	88	2	21	111
8	46	9	20	75
9	39	7	5	51
10	68	89	57	214
11	15	-	5	20
12	5	-	12	17
13	-	-	22	22
14	-	-	30	30
15	-	-	68	68
Avg. years considered	6.9	9.7	10.4	8.4

Table 2.
Mexican stations with highest WDR exposure (daDRI values).

Station	Region	Latitude (DD)	Longitude (DD)	Altitude (m)	daDRI ($m^2/s \cdot yr$)	max. $daDRI_\theta$ ($m^2/s \cdot yr$)
La Mina	Oaxaca	17.978	-96.109	20	22.52	15.48
ITESTA	Veracruz	21.334	-98.221	140	19.05	11.99
Cosamalopan	Veracruz	18.385	-95.807	12	17.67	11.54
La Posta	Veracruz	19.319	-96.329	7	14.20	10.55
Amatitlan	Veracruz	18.485	-95.713	612	12.34	6.47
Cerro Negro	Oaxaca	18.175	-96.285	35	8.05	5.27
La Granja	Veracruz	18.382	-96.241	40	7.80	7.31
El Porvenir	Oaxaca	17.451	-95.314	111	7.04	6.42
San Nicolás	Veracruz	18.790	-96.901	300	6.86	3.99
El Progreso	Oaxaca	17.526	-95.549	440	6.61	5.17

Table 3.
Mexican stations with highest DRWP exposure (dDRWP values).

Station	Region	Latitude (DD)	Longitude (DD)	Altitude (m)	dDRWP (Pa)	max. $dDRWP_{\theta}$ (Pa)
ITESTA	Veracruz	21.334	-98.221	140	238.50	266.39
La Granja	Veracruz	18.382	-96.241	40	181.63	211.78
Sagitario	Veracruz	21.823	-98.483	20	177.53	229.63
Álamo	Veracruz	20.934	-97.680	53	167.39	219.47
La Posta	Veracruz	19.319	-96.329	7	122.40	147.18
La Conquista	Veracruz	19.293	-96.379	58	67.97	62.61
El Tomatal	Oaxaca	15.797	-96.940	48	52.14	42.83
Tlacolula	Veracruz	21.091	-97.948	520	47.84	59.31
La Mina	Oaxaca	17.978	-96.109	20	45.56	40.51
Tepeaca	Puebla	18.989	-97.901	2235	43.58	39.05

Table 4.
Norwegian stations with highest WDR exposure (daDRI values).

Station	Region	Latitude (DD)	Longitude (DD)	Altitude (m)	daDRI ($m^2/s \cdot yr$)	max. $daDRI_\theta$ ($m^2/s \cdot yr$)
Ona II	More Og Romsdal	62.858	06.539	13	13.21	9.20
Nedre Vats	Rogaland	59.483	05.752	64	11.92	7.96
Lindesnes Fyr	Vest-Adger	57.981	07.048	16	11.92	6.02
Kvamskogen	Hordaland	60.387	05.965	455	11.90	7.03
Takle	Sogn og Fjordane	61.026	05.382	38	11.64	6.96
Utsira Fyr	Rogaland	59.305	04.873	55	11.49	6.94
Obrestad Fyr	Rogaland	58.658	05.556	24	11.05	5.93
Kvamsoy	Hordaland	60.362	06.281	49	10.71	7.39
Bergen-Florida	Hordaland	60.382	05.334	12	10.02	6.75
Lista Fyr	Vest-Adger	58.108	06.568	14	9.81	5.19

Table 5.
Norwegian stations with highest DRWP exposure (dDRWP values).

Station	Region	Latitude (DD)	Longitude (DD)	Altitude (m)	dDRWP (Pa)	max. $dDRWP_{\theta}$ (Pa)
Utsira Fyr	Rogaland	59.305	04.873	55	54.20	34.21
Lindesnes Fyr	Vest-Adger	57.981	07.048	16	54.18	43.33
Ona II	More Og Romsdal	62.858	06.539	13	53.75	50.58
Myken	Norland	66.761	12.486	17	51.30	36.75
Obrestad Fyr	Rogaland	58.658	05.556	24	39.62	32.76
Bjornoya	Svalbard	74.515	19.004	16	39.59	30.71
Lista Fyr	Vest-Adger	58.108	06.568	14	37.13	30.42
Torunger Fyr	Aust-Adger	58.397	08.790	12	36.99	27.22
Jan Mayen	Jan Mayen	70.939	-08.685	10	35.49	39.67
Kvitsoy-Nordbo	Rogaland	59.069	05.413	21	33.59	26.34

Table 6.
Spanish stations with highest WDR exposure (daDRI values).

Station	Region	Latitude (DD)	Longitude (DD)	Altitude (m)	daDRI ($m^2/s \cdot yr$)	max. $daDRI_\theta$ ($m^2/s \cdot yr$)
Machichaco	Basque Country	43.44	-02.76	433	11.29	7.65
La Cerroja	Basque Country	43.21	-03.41	677	9.63	8.64
Jaizquíbel	Basque Country	43.34	-01.86	545	9.37	7.23
Mt. Oiz	Basque Country	43.23	-02.60	980	7.86	5.33
Corrubedo	Galicia	42.56	-09.03	30	7.00	4.77
Bidania	Basque Country	43.14	-02.16	592	6.65	5.69
La Garbea	Basque Country	43.21	-03.19	717	6.24	4.36
Almike-Bermeo	Basque Country	43.41	-02.73	106	5.88	4.48
Iturrieta	Basque Country	42.79	-02.35	987	5.82	4.26
Soba-Alto Miera	Cantabria	43.19	-03.69	700	5.74	4.72

Table 7.
Spanish stations with highest DRWP exposure (dDRWP values).

Station	Region	Latitude (DD)	Longitude (DD)	Altitude (m)	dDRWP (Pa)	max. $dDRWP_{\theta}$ (Pa)
Machichaco	Basque Country	43.44	-02.76	433	51.80	46.07
Mt. Oiz	Basque Country	43.23	-02.60	980	43.27	41.32
Zaldiaran	Basque Country	42.79	-02.74	890	37.42	42.58
Jaizquíbel	Basque Country	43.34	-01.86	545	30.30	25.11
Kapildui radar	Basque Country	42.77	-02.54	1173	24.77	21.33
La Garbea	Basque Country	43.21	-03.19	717	24.53	19.58
Corrubedo	Galicia	42.56	-09.03	30	22.04	21.50
La Cerroja	Basque Country	43.21	-03.41	677	21.72	21.53
Róitegui	Basque Country	42.78	-02.37	980	19.76	17.89
Herrera	Basque Country	42.60	-02.68	1188	19.10	18.15

Table 8.
Distribution of analysed locations for different exposure ranges by country.

Exposure level	daDRI range ($m^2/s \cdot yr$)	Stations			Total (%)
		Mexico (%)	Spain (%)	Norway (%)	
Sheltered	≤ 3	481 (93.2)	254 (85.6)	51 (47.7)	786 (85.4)
Moderate	3 - 7	27 (5.2)	39 (13.1)	36 (33.6)	102 (11.1)
High	7 - 11	3 (0.6)	3 (1.0)	13 (12.1)	19 (2.1)
Severe	> 11	5 (1.0)	1 (0.3)	7 (6.6)	13 (1.4)

Exposure level	DRWP range (Pa)	Stations			Total (%)
		Mexico (%)	Spain (%)	Norway (%)	
Sheltered	≤ 8.5	459 (89.0)	267 (89.9)	59 (55.1)	785 (85.3)
Moderate	8.5 - 30	41 (7.9)	26 (8.8)	35 (32.7)	102 (11.1)
High	30 - 45.0	7 (1.4)	3 (1.0)	9 (8.4)	19 (2.1)
Severe	> 45.0	9 (1.7)	1 (0.3)	4 (3.8)	14 (1.5)

Table 9.
Scalar and maximum directional WDR exposures calculated using ISO standard 15927-3 for Northwestern Spain (Galicia region).

Location	Latitude (DD)	Longitude (DD)	Altitude (m)	WDR (mm/yr)	Max. WDR_θ (mm/yr)
Lousame	42.75	-08.78	661	4958.90	3994.45
Fornelos de Montes	42.31	-08.40	705	3860.48	3054.98
Manzaneda	42.26	-07.30	1758	2743.12	1985.14
Santa Comba	42.97	-08.87	369	2508.10	1794.23
Rodeiro	42.58	-07.93	842	2634.11	1793.92
Oia	41.99	-08.87	473	2386.12	1647.89
Monfero	43.34	-07.89	651	2377.46	1588.41
Tui	42.08	-08.68	484	1683.48	1502.05
Ribeira	42.46	-09.01	24	2011.96	1410.62
Maceda	42.30	-07.59	981	1655.39	1374.09
…					
Viana do Bolo	42.16	-07.09	851	682.03	549.85
Celanova	42.17	-07.97	623	772.87	544.45
Lalín	42.61	-08.14	500	843.84	504.98
Abegondo	43.24	-08.26	94	710.62	502.57
Ribadeo	43.54	-07.08	51	768.62	477.69
Ferrol	43.49	-08.25	37	981.73	392.75
Monforte de Lemos	42.47	-07.50	645	581.53	382.66
Pontevedra	42.41	-08.66	57	591.52	328.15
Lugo	42.99	-07.55	400	461.30	262.30
Verín	41.97	-07.40	546	441.74	255.16

Supplementary material (Excel file)

Avoiding the need to directionally determine the exposure to rainwater penetration for facade designs

Building and Environment

J.M. Pérez-Bella; J. Domínguez-Hernández; E. Cano-Suñén; J.E. Martínez-Martínez; J.J. del Coz-Díaz

Corresponding author: *José M. Pérez-Bella. Department of Construction Engineering, University of Zaragoza, Campus Río Ebro, Edificio Betancourt, María de Luna s/n, 50018, Zaragoza, Spain. E-mail: jmpb@unizar.es*

Scalar and maximum directional values of WDR exposure calculated by standard ISO 15927-3 in Northwestern Spain (complete Table 9):

	Buenavista del Norte (Canary Islands)						
Region	**Location**	**Latitude (Decimal Degrees)**	**Longitude (DD)**	**Years considered**	**Dataset time resolution**	**Scalar WDR (mm/yr)**	**Maximum WDR$_\theta$ (mm/yr)**
GALICIA	LOUSAME	42,7456	-08,7763	10	hourly	4958,90	3994,45
GALICIA	FORNELOS DE MONTES	42,3153	-08,4002	10	hourly	3860,48	3054,98
GALICIA	MANZANEDA	42,2602	-07,2983	10	hourly	2743,12	1985,14
GALICIA	SANTA COMBA	42,9686	-08,8683	10	hourly	2508,10	1794,23
GALICIA	RODEIRO	42,5798	-07,9331	10	hourly	2634,11	1793,92
GALICIA	OIA	41,9945	-08,8662	10	hourly	2386,12	1647,89
GALICIA	MONFERRO	43,3431	-07,8944	10	hourly	2377,46	1588,41
GALICIA	TUI	42,0786	-08,6795	10	hourly	1683,48	1502,05
GALICIA	RIBEIRA	42,4649	-09,0136	10	hourly	2011,96	1410,62
GALICIA	MACEDA	42,2987	-07,5907	10	hourly	1655,39	1374,09
GALICIA	FRAGAVELLA	43,4546	-07,4463	10	hourly	2160,59	1363,20
GALICIA	CASTROVE	42,4593	-08,7043	10	hourly	1701,22	1342,57
GALICIA	ONS	42,3821	-08,9362	10	hourly	1880,04	1322,09
GALICIA	LARDEIRA	42,3752	-06,7835	10	hourly	1872,95	1290,11
GALICIA	CORÓN	42,5801	-08,8047	10	hourly	1644,80	1156,91
GALICIA	CORRUBEDO	42,5552	-08,0286	10	hourly	1557,04	1154,18
GALICIA	MALPICA	43,3360	-08,8364	10	hourly	1653,02	1152,75
GALICIA	PUNTA CANDEIRA	43,7043	-08,0525	10	hourly	1640,04	1108,77
GALICIA	GUITIRIZ	43,2266	-07,7831	10	hourly	1364,22	1036,38
GALICIA	SANTIAGO EOAS	42,8760	-08,5594	10	hourly	1233,48	1029,67
GALICIA	ANCARES	42,8208	-06,9229	10	hourly	1671,80	993,58
GALICIA	XARES	42,2078	-06,8926	10	hourly	1526,13	934,49
GALICIA	VENTOSA	42,9560	-06,9153	10	hourly	1208,58	919,99
GALICIA	ILLAS CIES	42,2118	-08,9084	10	hourly	1022,78	874,80
GALICIA	O XIPRO	43,1771	-07,0479	10	hourly	1089,97	703,24
GALICIA	BURELA	43,6449	-07,3748	10	hourly	1376,66	684,35
GALICIA	SANXENXO	42,4031	-08,7988	10	hourly	883,83	647,32
GALICIA	O INVERNADEIRO	42,1196	-07,3446	10	hourly	1111,04	634,60
GALICIA	QUEIMADELOS	42,2253	-08,4285	10	hourly	686,60	586,78
GALICIA	MELIDE	42,9074	42,9074	10	hourly	854,86	579,05
GALICIA	VIANA DO BOLO	42,1630	-07,0896	10	hourly	682,03	549,85
GALICIA	CELANOVA	42,1736	-07,9682	10	hourly	772,87	544,45
GALICIA	LALÍN	42,6144	-08,1373	10	hourly	843,84	504,98
GALICIA	ABEGONDO	43,2414	-08,2622	10	hourly	710,62	502,57
GALICIA	RIBADEO	43,5407	-07,0830	10	hourly	768,62	477,69
GALICIA	FERROL	43,4915	-08,2523	10	hourly	981,73	392,75
GALICIA	MONFORTE DE LEMOS	42,4732	-07,5018	10	hourly	581,53	382,66
GALICIA	PONTEVEDRA	42,4092	-08,6642	10	hourly	591,52	328,15
GALICIA	LUGO	42,9927	-07,5469	10	hourly	461,30	262,30
GALICIA	VERÍN	41,9743	-07,3988	10	hourly	441,74	255,16

Figure captions

Figure 1. Example of differences in the directional exposure for two weather stations analysed in this study (Itesta and La Posta, both in Mexico); angles are measured in degrees from the North.

Figure 2. Geographical scope of this study: analysed stations are shown by crosses.

Figure 3. Best-fit correlation between scalar and maximum directional exposures for 920 analysed locations. *Percent error range of ± 20% is also shown.*

Figure 4. Best-fit correlation between scalar and maximum directional exposures by country.

Figure 5. Best-fit correlation between scalar and maximum directional WDR exposures for 40 Spanish sites based on hourly data (according to ISO 15927-3). *Percent error range of ± 20% is also shown.*

Figure 1

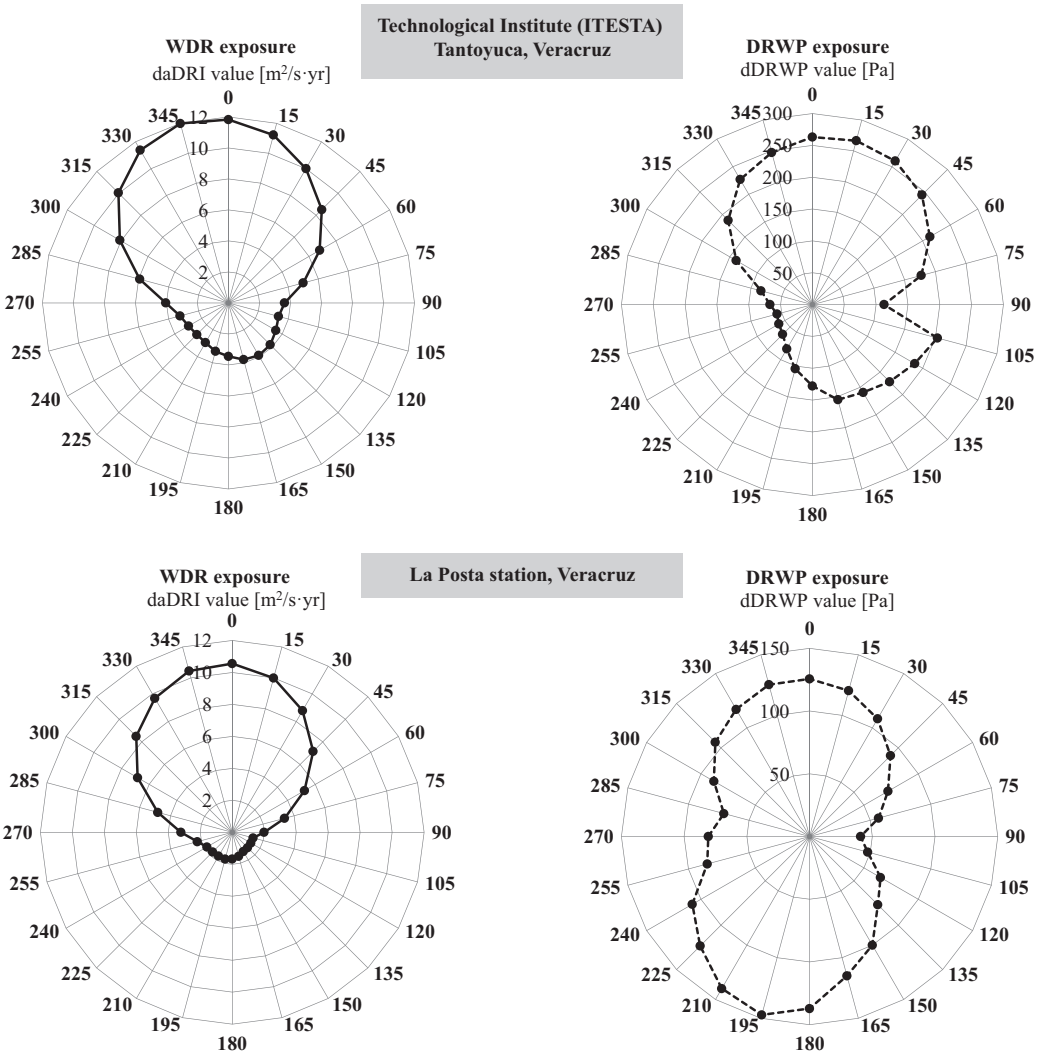

Figure 1. Example of differences in the directional exposure for two weather stations analysed in this study (Itesta and La Posta, both in Mexico); angles are measured in degrees from the North.

Figure 2

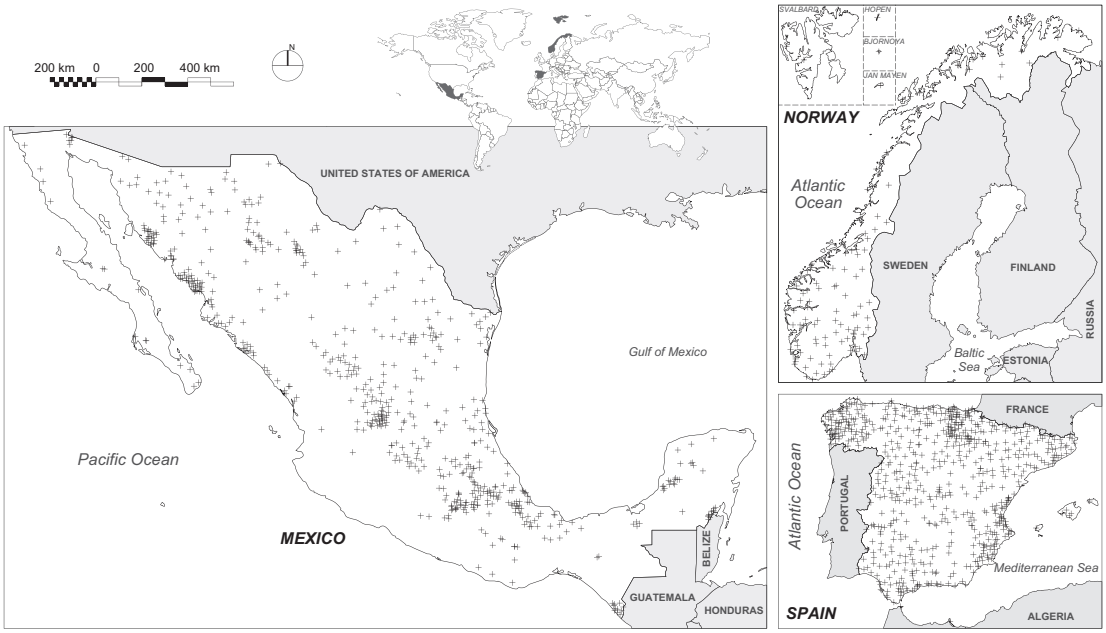

Figure 2. Geographical scope of this study: analysed stations are shown by crosses.

Figure 3

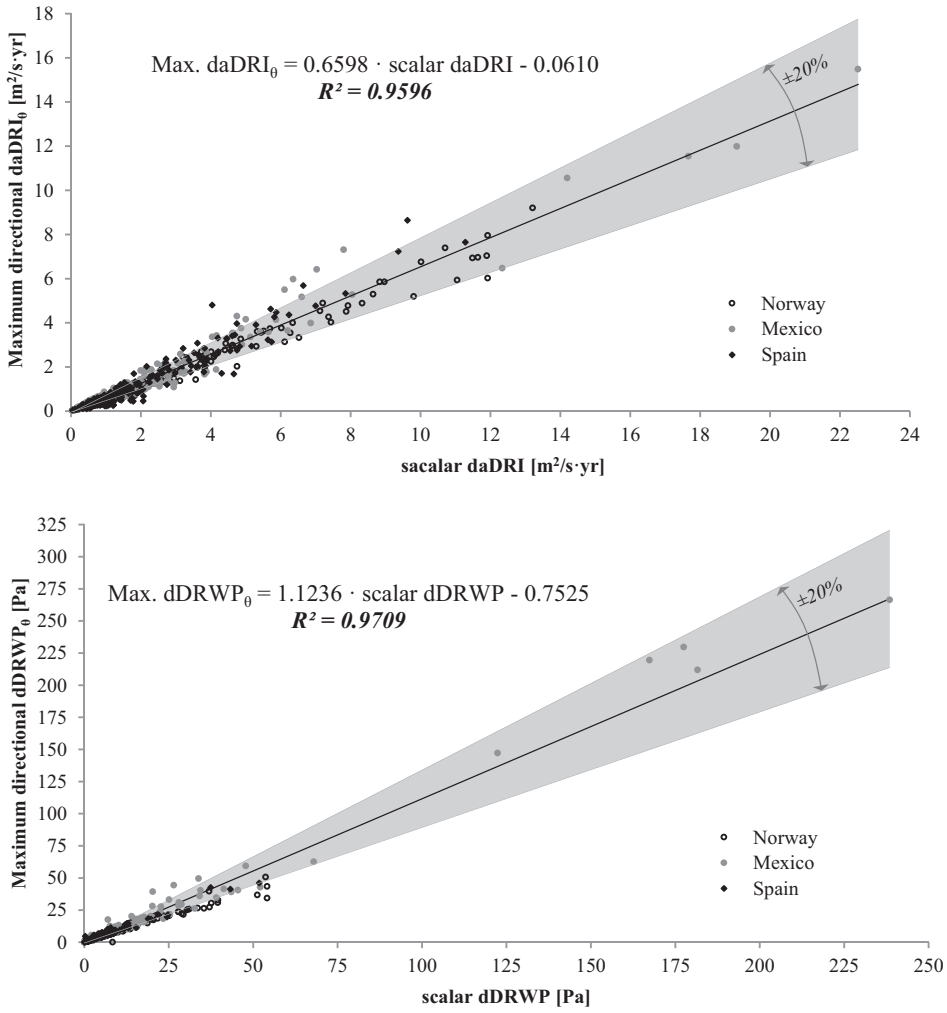

Figure 3. Best-fit correlation between scalar and maximum directional exposures for 920 analysed locations. *Percent error range of ±20% is also shown.*

Figure 4

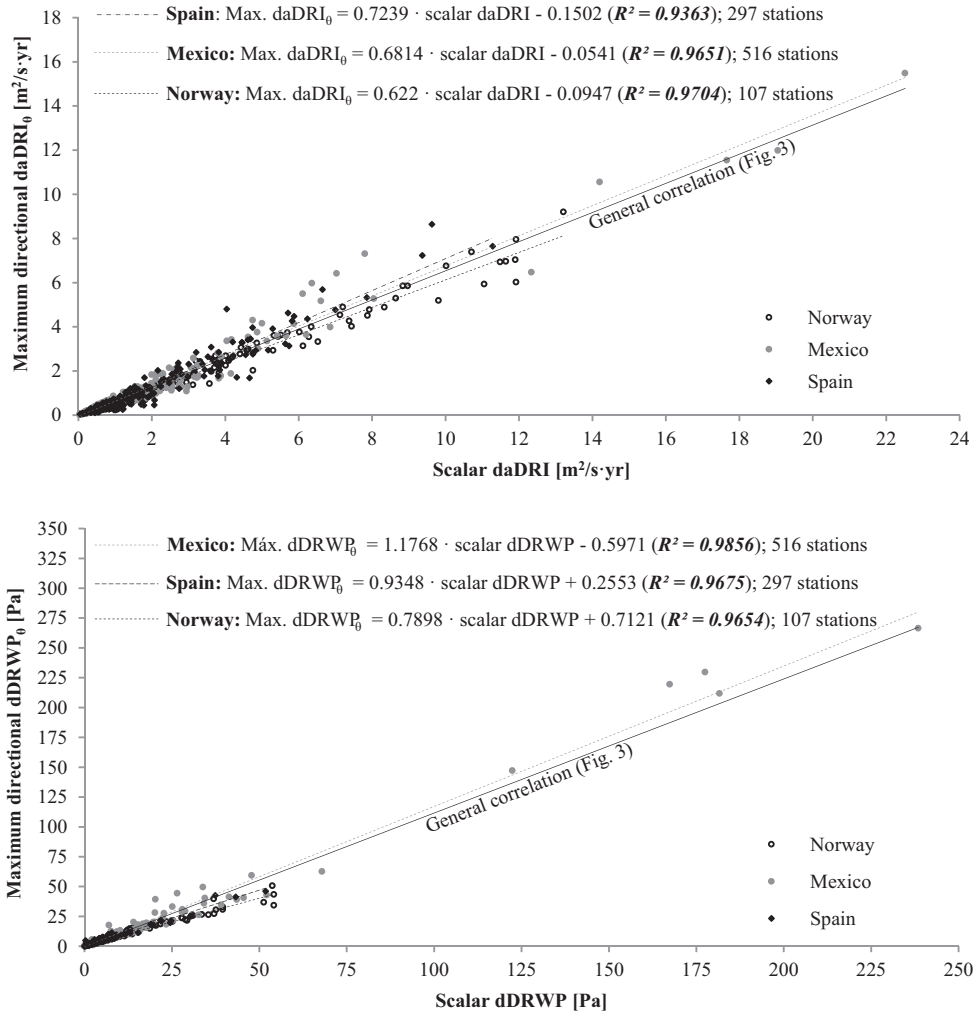

Figure 4. Best-fit correlation between scalar and maximum directional exposure by country.

Figure 5

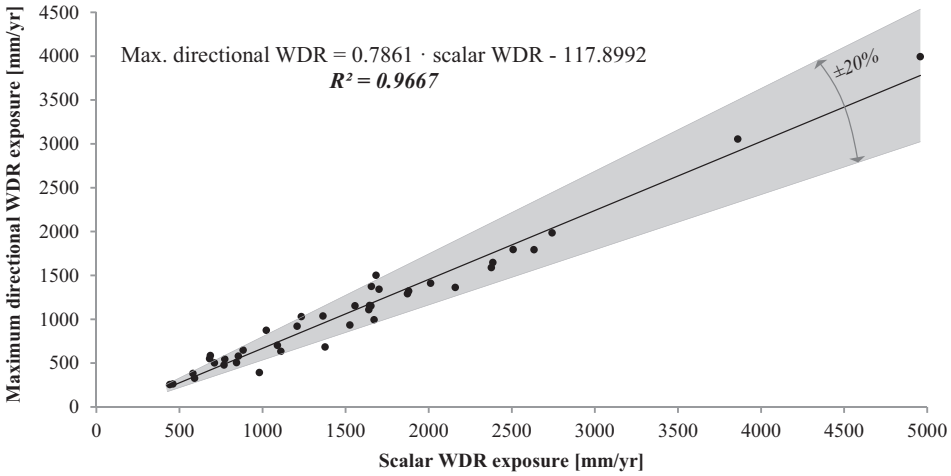

Figure 5. Best-fit correlation between scalar and maximum directional WDR exposures for 40 Spanish sites based on hourly data (according to ISO 15927-3).
Percent error range of ±20% is also shown.